Two different routes to chaos in a two-mode CO_2 laser with a saturable absorber

Kazuhito Tanii,[1,*] Takehisa Tohei,[2,†] Toshiki Sugawara,[3,‡] Maki Tachikawa,[4,§] and Tadao Shimizu[5,‖]
[1]*Department of Electronics, Chiyoda College of Art and Engineering, 1-5-30 Sitaya, Taito-ku, Tokyo 110-0004, Japan*
[2]*Department of Applied Physics, Science University of Tokyo, 1-3 Kagurazaka, Shinjuku-ku, Tokyo 162-0825, Japan*
[3]*Optoelectronics Research Department, Hitachi Ltd., 1-280 Higashi-koigakubo, Kokubunji, Tokyo 185-0014, Japan*
[4]*Department of Physics, Meiji University, 1-1-1 Higashimita, Tama-ku, Kawasaki, Kanagawa 214-0033, Japan*
[5]*Department of Electronics and Computer Science, Science University of Tokyo in Yamaguchi, 1-1-1 Daigaku-dori, Onoda, Yamaguchi 756-0884, Japan*
(Received 30 June 1998)

Instabilities in a two-mode CO_2 laser with an intracavity saturable absorber are investigated both theoretically and experimentally. In addition to the period-doubling route to chaos, the intermittency route to chaos is induced by the cross saturation between the two oscillating modes. The strange attractor of the intermittent chaos observed in this laser system has a higher fractal dimension than that of the chaos associated with the period-doubling bifurcation. [S1063-651X(99)07502-9]

PACS number(s): 05.45.−a, 42.55.Lt, 42.65.Sf

A laser is a useful model for studying various aspects of nonlinear dynamics. Deterministic chaos and bifurcations were observed in simple laser systems such as a Lorenz-type laser [1,2] and a laser with parameter modulation [3,4]. Recent investigations focus on more complex behavior when extra degrees of freedom are introduced to the laser, or the optical elements are coupled to each other. Multimode or coupled lasers show various effects such as in-phase or antiphase dynamics [5–10], spatiotemporal dynamics [10–17], gain circulation [18], phase locking [19–21], periodic mode alternation governed by the Farey arithmetic [22,23], and synchronization [24–28].

In our previous paper [5], we reported instabilities in a multimode CO_2 laser containing a saturable absorber inside its cavity. The laser oscillation occurs on two different lines, one is in the axial transverse electric and magnetic (TEM_{00}) mode, and the other is in the off-axial TEM_{01} mode. Only the line in the axial mode is passively Q switched (PQS) by the saturable absorber. The introduction of the extra lasing mode makes the laser dynamics much richer than the single-mode PQS instability. Our analysis revealed that this laser shows alternate switching between the two modes and simultaneous oscillation, depending on the system parameters. This rate-equation model predicted the existence of chaos which has a higher-dimensional attractor than in the case of single-mode chaotic PQS pulsation [29–32].

In this paper, we investigate more details of the two-mode chaos. The theoretical model predicts that there are two types of chaotic pulsation, one associated with the intermittency route and the other with period-doubling bifurcation. Characteristics of the intermittent chaos are clarified in the rate-equation analysis using Poincaré sections and first return maps. The existence of these two different routes to chaos is experimentally demonstrated in a CO_2 laser with a formic acid saturable absorber.

Based on our model, the laser system is described by a set of seven nonlinear rate equations taking into account the cross saturation between the two modes due to spatial overlap [5]:

$$\frac{dn_c}{dt}=B_g n_c f_g(J)(M_{c1}-M_{c2})l_g/L+C_1B_g n_c f_g(J)\times(M_{s1}-M_{s2})l_g/L-B_aNn_c l_a/L-k_c n_c, \tag{1}$$

$$\frac{dn_s}{dt}=B_g n_s f_g(J')(M_{s1}-M_{s2})l_g/L+C_2B_g n_s f_g(J')\times(M_{c1}-M_{c2})l_g/L-k_s n_s, \tag{2}$$

$$\frac{dM_{c1}}{dt}=-B_g n_c f_g(J)(M_{c1}-M_{c2})-C_2B_g n_s f_g(J')\times(M_{c1}-M_{c2})+P_c(M_c-M_{c1}-M_{c2})-(R_{10}+R_{12})M_{c1}+R_m(M_{s1}-M_{c1}), \tag{3}$$

$$\frac{dM_{c2}}{dt}=B_g n_c f_g(J)(M_{c1}-M_{c2})+C_2B_g n_s f_g(J')\times(M_{c1}-M_{c2})-R_{20}M_{c2}+R_{12}M_{c1}+R_m(M_{s2}-M_{c2}), \tag{4}$$

$$\frac{dM_{s1}}{dt}=-B_g n_s f_g(J')(M_{s1}-M_{s2})-C_1B_g n_c f_g(J)\times(M_{s1}-M_{s2})+P_s(M_s-M_{s1}-M_{s2})-(R_{10}+R_{12})M_{s1}+R_m(M_{c1}-M_{s1}), \tag{5}$$

*Electronic address: jp002741@jp.interramp.com
†Electronic address: tohei@rs.kagu.sut.ac.jp
‡Electronic address: t-suga@crl.hitachi.co.jp
§Electronic address: tachikaw@isc.meiji.ac.jp
‖Electronic address: tshimizu@ke.yama.sut.ac.jp

$$\frac{dM_{s2}}{dt}=B_g n_s f_g(J')(M_{s1}-M_{s2})+C_1 B_g n_c f_g(J)\times(M_{s1}-M_{s2})-R_{20}M_{s2}+R_{12}M_{s1}+R_m(M_{c2}-M_{s2}), \quad (6)$$

$$\frac{dN}{dt}=-2B_a n_c N-r(N-N^*). \quad (7)$$

Here n_c (n_s) is the mean photon density of the TEM_{00} (TEM_{01}) mode in the center (side) region of the laser gain medium. M_{c1} (M_{s1}) and M_{c2} (M_{s2}) are, respectively, the population densities of the upper and lower laser levels in the center (side) region. N is the population density difference between the absorber levels. The coupling constants C_1 and C_2 are determined by the transverse intensity distribution of the TEM_{00} and TEM_{01} modes. R_m is the rate constant for diffusion of CO_2 molecules between the center and side regions. Notations of the other parameters are identical with those of the rate-equation model for the single-mode laser [30], although the subscripts c and s, respectively, indicate the parameters in the center and side regions, and J (J') indicates the rotational quantum number of the laser line in the axial (off-axial) mode.

According to the numerical simulation on this rate-equation model, there are two different regions in the parameter space where chaotic two-mode pulsation appears (see Fig. 3 of Ref. [5]). It is shown in further analysis that, in one region, chaos occurs after period-doubling bifurcation when a parameter is varied. The intermittency route to chaos appears in the other region. Figures 1(a)–1(d) show the period-doubling route to chaos numerically calculated for the parameter values in Table I. These parameter values are reasonable for the present laser system [5]. Pumping rates, P_c and P_s, are varied as control parameters. Here P_c is assumed to equal P_s. In the periodic state, pulsations of the two modes are synchronized, and their period is successively doubled as the pumping rate is increased. The return map for the chaotic pulsation in the axial mode (TEM_{00}) in Fig. 1(d) is shown in Fig. 1(e), in which the $(n+1)$th peak value of the pulse train is plotted as a function of the nth peak.

For another set of parameter values of the saturable absorber listed in Table I, the two-mode laser exhibits the intermittency route to chaos with an increase in the pumping rate P_c ($=P_s$), as shown in Figs. 2(a)–2(c). With an increase in the pumping rate, the regular pulsation becomes unstable and chaotic bursts take place more frequently. The bursts are simultaneously observed in both modes. The return map for the axial mode pulsation in Fig. 2(b) is shown in Fig. 2(d). There is an unstable fixed point in the open-circle area of the return map. Once the peak value comes into the vicinity of the unstable fixed point, it rotates around and gradually deviates from the point. This corresponds to the pulse-height modulation before the burst [see Fig. 2(b)].

The Poincaré section in Fig. 3, on which the TEM_{00} mode photon density takes its peak value, shows successive cross points when the trajectory circulates around the fixed point. The coordinates x and y are defined as

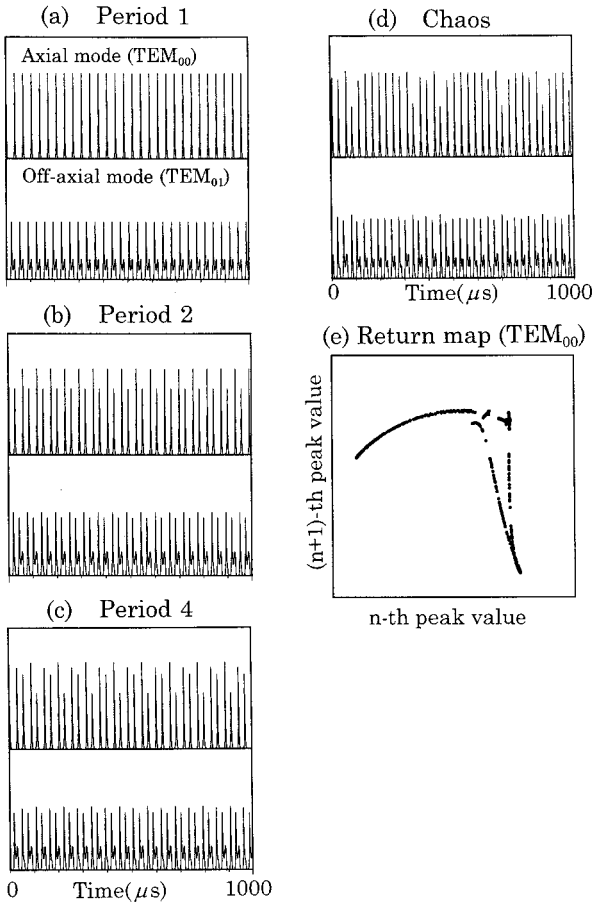

FIG. 1. Calculated PQS pulse trains [(a)–(d)] as functions of the pumping rate P_c ($=P_s$). The upper and the lower pulse trains are of n_c (TEM_{00} mode) and n_s (TEM_{01} mode), respectively. The period-doubling route to chaos occurs as the pumping rate is increased [(a) $P_c=26.0$ Hz, (b) $P_c=30.2$ Hz, (c) $P_c=30.6$ Hz, (d) $P_c=31.0$ Hz]. The return map of the chaotic axial mode pulsation in (d) is shown in (e).

$$x=-4.6[n_c-n_c(0)]-7.7[M_{c1}-M_{c2}-M_{c1}(0)+M_{c2}(0)], \quad (8)$$

$$y=-0.51[M_{c1}-M_{c2}-M_{c1}(0)+M_{c2}(0)]+0.86[n_c-n_c(0)], \quad (9)$$

TABLE I. Parameter values used in the numerical calculations.

Parameters		Fig. 1	Fig. 2
R_{10}	$[10^3/s]$	1.0	1.0
R_{20}	$[10^6/s]$	0.38	0.38
R_{12}	$[10^3/s]$	0.2	0.2
$B_g f_g(J) M_c l_g/L$	$[10^6/s]$	4300	4300
$B_g f_g(J') M_s l_g/L$	$[10^6/s]$	3900	3900
k_c	$[10^6/s]$	2.5	2.5
k_s	$[10^6/s]$	3.5	3.5
r	$[10^6/s]$	13.42	18.0
$B_a N^* l_a/L$	$[10^6/s]$	1.9	1.4
$B_a/B_g f_g(J)$		303.73	301.66
C_1, C_2		0.26	0.26

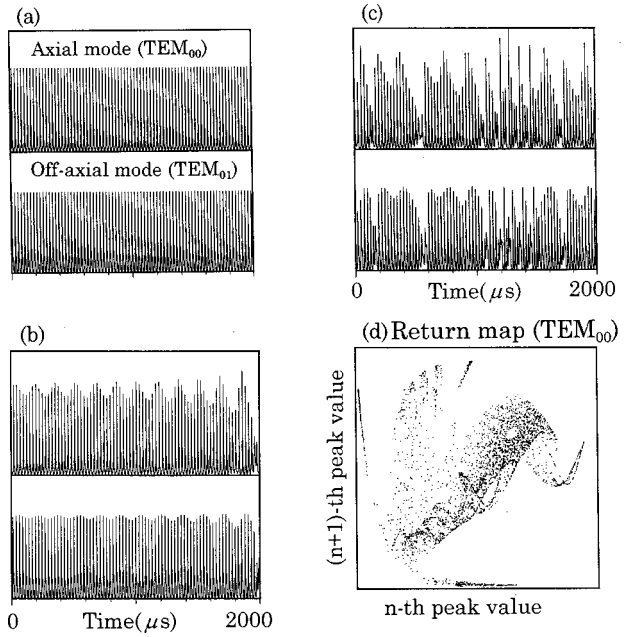

FIG. 2. Intermittency route to chaos numerically calculated with an increase in the pumping rate [(a) $P_c = 24.800$ Hz, (b) $P_c = 24.832$ Hz, (c) $P_c = 24.834$ Hz]. The return map of the chaotic axial mode pulsation in (c) is shown in (d).

where $n_c(0)$, $M_{c1}(0)$, and $M_{c2}(0)$ are estimated values for the unstable fixed point. The data point travels around the fixed point counterclockwise. The distance from the fixed point gradually amplifies until the pulsation turns into the chaotic burst, which represents that this intermittency belongs to type II.

The return map of the chaotic pulsation associated with the period doubling traces nearly one-dimensional curves. On the other hand, data points in the return map for the intermittency are distributed two dimensionally. The fractal dimension of the strange attractors is measured with the Grassberger and Proccacia technique [33] to be 2.02 ± 0.02 for the calculated chaotic time series with period doubling, and 2.47 ± 0.01 for the intermittent chaos. The fact that the dimension of the period-doubling case is close to 2 is consistent with the one-dimensional structure in the return map for the period-doubling case.

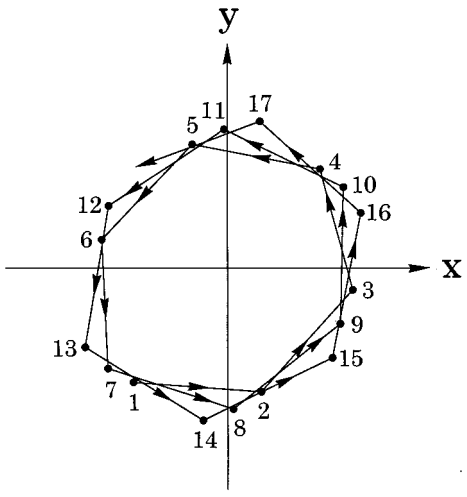

FIG. 3. Intersections of the trajectory around the unstable fixed point in the Poincaré section. The intersections are numbered according to the order of time evolution.

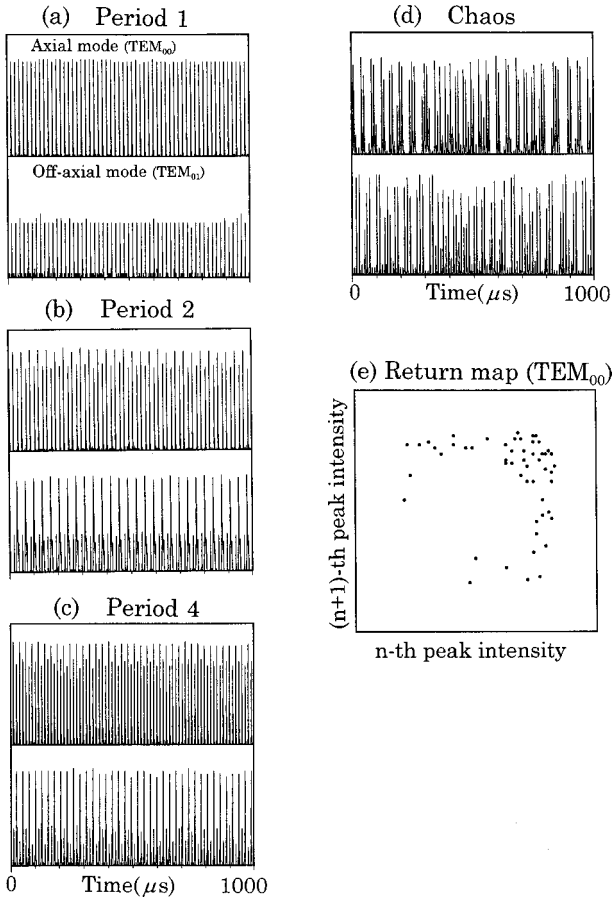

FIG. 4. Observed PQS pulse trains [(a)–(d)] as functions of the discharge current [(a) 4.5 mA, (b) 4.8 mA, (c) 5.1 mA, (d) 6.8 mA]. The upper and the lower pulse trains are of the TEM_{00} mode and TEM_{01} mode, respectively. The period-doubling route to chaos occurs as the pumping rate is increased. The return map of the chaotic axial mode pulsation in (d) is shown in (e).

Two different routes to chaos are experimentally observed using a two-mode CO_2 laser with a formic acid absorber. Detailed experimental setup of the CO_2 laser system is described elsewhere [29,30]. In brief, two irises placed inside the laser cavity are opened up to 15 mm in diameter for two-mode oscillation. TEM_{00} and TEM_{01} modes are selected by fine adjustment of the cavity alignment. The axial mode oscillates on a 9-μm $R(18)$ line, and the off-axial mode on a 9-μm $R(24)$ line. The output radiation is split into two beams, and then fed into monochromators; one is tuned to the $R(18)$ line, and the other to the $R(24)$ line. The laser intensity on each mode is detected by a HgCdTe detector after the monochromator.

The period-doubling route, chaotic pulsations, and its return map are shown in Fig. 4. The absorber pressure is 62 mTorr, and 1.43 Torr of SF_6 is added to the absorber as a buffer gas. The intermittency route is also observed when the absorber conditions are carefully adjusted (see Fig. 5). In this case, the absorber pressure is 21 mTorr, and methanol is used as a buffer gas at the pressure of 216 mTorr. In experiment, the regular part of the time sequence consists of triple-

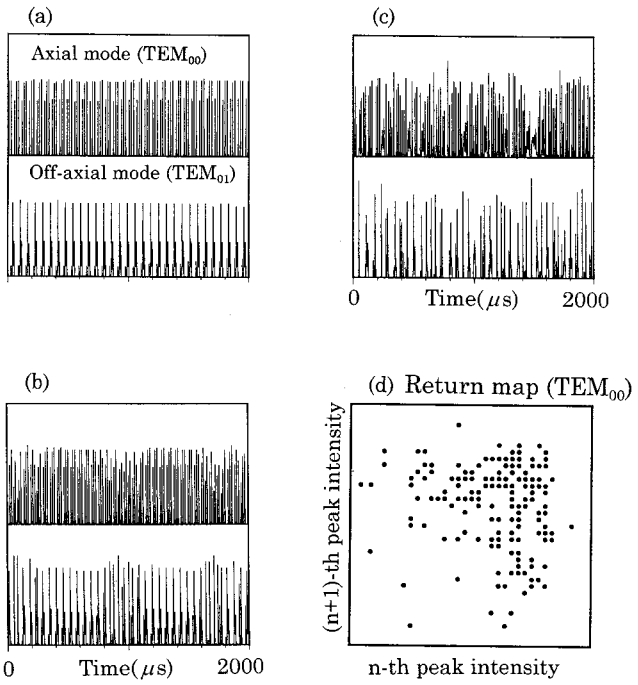

FIG. 5. Intermittency route to chaos experimentally observed with a slight increase in the discharge current. The return map of the chaotic axial mode pulsation in (c) is shown in (d).

peaked pulses in contrast to the single-peaked pulses in Fig. 2. This pulse train can be reproduced in the numerical simulation with a slightly different parameter set.

The difference in structure of strange attractors between the two types of chaotic pulsation is confirmed from experimentally obtained return maps. In the return map for the chaotic pulsation observed after period doubling [Fig. 4(e)], data points are localized in the neighborhood of the theoretically predicted one-dimensional curves. In the return map for the observed intermittency [Fig. 5(d)], however, data points are two-dimensionally distributed over a wider area.

Even in the absence of the off-axial mode, this CO_2 laser system exhibits chaotic passively *Q*-switched pulsation led by the period-doubling bifurcation. The single-mode chaos has a strange attractor with a fractal dimension of 2.01 ± 0.01, and its return map traces a one-dimensional curve [5]. This correspondence between the single-mode chaos and the two-mode chaos with the lower dimension implies that the off-axial mode variables are not working as independent degrees of freedom in the case of the two-mode chaos led by the period-doubling bifurcation. On the other hand, in the case of the intermittency, the introduction of the extra lasing mode makes the laser instability more complicated through the cross saturation dynamics, yielding the strange attractor with a higher fractal dimension and two-dimensional distribution in the return maps. Further experiment and analysis are in progress to identify that the observed intermittency belongs to type II.

In conclusion, two different routes to chaos in the two-mode CO_2 laser with a saturable absorber were predicted on the basis of the rate-equation model, and their existence has been experimentally confirmed. The present model quite well describes the population dynamics in the multimode laser, and may be applied to higher-dimensional systems.

This work is supported by a Grant-in-Aid for Project Research (B) (2) 08455040 from the Ministry of Education, Science, and Culture.

[1] C. O. Weiss, N. B. Abraham, and U. Hubner, Phys. Rev. Lett. **61**, 1587 (1988).
[2] H. Zeghlache, P. Mandel, N. B. Abraham, and C. O. Weiss, Phys. Rev. A **38**, 3128 (1988).
[3] F. T. Arrecchi, R. Meucci, G. Puccioni, and J. Tredicce, Phys. Rev. Lett. **49**, 1217 (1982).
[4] F. T. Arrecchi, W. Gadomski, and R. Meucci, Phys. Rev. A **34**, 1617 (1986).
[5] K. Tanii, M. Tachikawa, T. Tohei, F.-L. Hong, and T. Shimizu, Phys. Rev. A **43**, 1498 (1991).
[6] P. Hadley and M. R. Beasley, Appl. Phys. Lett. **50**, 621 (1987).
[7] K. Otsuka, M. Georgiu, and P. Mandel, Jpn. J. Appl. Phys., Part 1 **31**, L1250 (1992).
[8] P. Mandel, M. Georgiu, K. Otsuka, and D. Pieroux, Opt. Commun. **100**, 241 (1993).
[9] D. Y. Tang, R. Dykstra, and N. R. Heckenberg, Phys. Rev. A **54**, 5317 (1996).
[10] D. Wilkowski, D. Hennequin, D. Dangoisse, and P. Glorieux, Chaos Solitons Fractals **4**, 1683 (1994).
[11] F. Papof, G. D'Alessandro, G-L. Oppo, and W. J. Firth, Phys. Rev. A **48**, 634 (1993).
[12] K. Otsuka, D. Pieroux, and P. Mandel, Opt. Commun. **108**, 265 (1994).
[13] D. Pieroux, P. Mandel, and K. Otsuka, Opt. Commun. **108**, 273 (1994).
[14] B. M. Jost and B. E. A. Saleh, Phys. Rev. A **51**, 1539 (1995).
[15] L. M. Hoffer, G. L. Lippi, J. Narik, Ch. Vorgerd, and W. Lange, in *Nonlinear Dynamics in Optical Systems Technical Digest, 1992* (Optical Society of America, Washington, D.C., 1992), Vol. 16, pp. 229–231.
[16] M. Vaupel and C. O. Weiss, Phys. Rev. A **51**, 4078 (1995).
[17] M. Vaupel, K. Staliunas, and C. O. Weiss, Phys. Rev. A **54**, 880 (1996).
[18] K. Otsuka and Y. Aizawa, Phys. Rev. Lett. **72**, 2701 (1994).
[19] A. A. Golubentsev and V. V. Likhanskii, IEEE J. Quantum Electron. **17**, 592 (1990).
[20] S. N. Kozlov and V. V. Likhanskii, Laser Phys. **3**, 1067 (1993).
[21] S. Yu. Kourtchatov, V. V. Likhanskii, A. P. Napartovich, F. T. Arecchi, and Lapucci, Phys. Rev. A **52**, 4089 (1995).
[22] D. Hennequin, D. Dangoisse, and P. Glorieux, Opt. Commun. **79**, 200 (1990).
[23] D. Hennequin, D. Dangoisse, and P. Glorieux, Phys. Rev. A **42**, 6966 (1990).
[24] R. Meucci, W. Gadomski, M. Ciofini, and F. T. Arrecci, Phys. Rev. E **49**, R2528 (1994).
[25] N. Watanabe and K. Karaki, Opt. Lett. **20**, 1032 (1995).

[26] T. Sugawara, M. Tachikawa, T. Tsukamoto, and T. Shimizu, Phys. Rev. Lett. **72**, 3502 (1994).
[27] Y. Liu, P. C. de Oliveira, M. B. Danailov, and J. R. Rios Leite, Phys. Rev. A **50**, 3464 (1994).
[28] T. Tsukamoto, M. Tachikawa, T. Hirano, T. Kuga, and T. Shimizu, Phys. Rev. E **54**, 4476 (1996).
[29] M. Tachikawa, K. Tanii, M. Kajita, and T. Shimizu, Appl. Phys. B: Photophys. Laser Chem. **39**, 83 (1986).
[30] M. Tachikawa, K. Tanii, and T. Shimizu, J. Opt. Soc. Am. B **4**, 387 (1987).
[31] M. Tachikawa, K. Tanii, and T. Shimizu, J. Opt. Soc. Am. B **5**, 1077 (1988).
[32] M. Tachikawa, F-L. Hong, K. Tanii, and T. Shimizu, Phys. Rev. Lett. **22**, 2266 (1988).
[33] P. Grassberger and I. Procaccia, Phys. Rev. A **28**, 2591 (1983).